



VICTORIA UNIVERSITY
MELBOURNE AUSTRALIA

A Machine Learning Model for Predicting Critical Minimum Foot Clearance (MFC) Heights

This is the Published version of the following publication

Nagano, Hanatsu, Prokofieva, Maria, Asogwa, Clement, Sarashina, Eri and Begg, Rezaul (2024) A Machine Learning Model for Predicting Critical Minimum Foot Clearance (MFC) Heights. *Applied Sciences*, 14 (15). ISSN 2076-3417

The publisher's official version can be found at
<https://www.mdpi.com/2076-3417/14/15/6705>
Note that access to this version may require subscription.

Downloaded from VU Research Repository <https://vuir.vu.edu.au/49154/>

Article

A Machine Learning Model for Predicting Critical Minimum Foot Clearance (MFC) Heights

Hanatsu Nagano ^{1,*} , Maria Prokofieva ¹ , Clement Ogugua Asogwa ¹, Eri Sarashina ² and Rezaul Begg ^{1,*} ¹ Institute for Health and Sport (IHES), Victoria University, Melbourne, VIC 8001, Australia² Graduate School of Comprehensive Human Sciences, Faculty of Health and Sport Sciences, University of Tsukuba, Tsukuba 305-8577, Japan

* Correspondence: hanatsu.nagano@vu.edu.au (H.N.); rezaul.begg@vu.edu.au (R.B.)

Featured Application: The machine learning model predicts Minimum Foot Clearance heights to prevent tripping falls. Integrated into exoskeletons or other assistive devices, it offers real-time interventions for vulnerable populations, enhancing safety with quick and accurate foot clearance adjustments.

Abstract: Tripping is the largest cause of falls, and low swing foot ground clearance during the mid-swing phase, particularly at the critical gait event known as Minimum Foot Clearance (MFC), is the major risk factor for tripping-related falls. Intervention strategies to increase MFC height can be effective if applied in real-time based on feed-forward prediction. The current study investigated the capability of machine learning models to classify the MFC into various categories using toe-off kinematics data. Specifically, three MFC sub-categories (less than 1.5 cm, between 1.5 and 2.0 cm, and higher than 2.0 cm) were predicted to apply machine learning approaches. A total of 18,490 swing phase gait cycles' data were extracted from six healthy young adults, each walking for 5 min at a constant speed of 4 km/h on a motorized treadmill. K-Nearest Neighbor (KNN), Random Forest, and XGBoost were utilized for prediction based on the data from toe-off for five consecutive frames (0.025 s duration). Foot kinematics data were obtained from an inertial measurement unit attached to the mid-foot, recording tri-axial linear accelerations and angular velocities of the local coordinate. KNN, Random Forest, and XGBoost achieved 84%, 86%, and 75% accuracy, respectively, in classifying MFC into the three sub-categories with run times of 0.39 s, 13.98 s, and 170.98 s, respectively. The KNN-based model was found to be more effective if incorporated into an active exoskeleton as the intelligent system to control MFC based on the preceding gait event, i.e., toe-off, due to its quicker computation time. The machine learning-based prediction model shows promise for the prediction of critical MFC data, indicating higher tripping risk.

Keywords: minimum foot clearance (MFC); tripping prevention; falls prevention; machine learning; gait prediction

check for
updates

Citation: Nagano, H.; Prokofieva, M.; Asogwa, C.O.; Sarashina, E.; Begg, R. A Machine Learning Model for Predicting Critical Minimum Foot Clearance (MFC) Heights. *Appl. Sci.* **2024**, *14*, 6705. <https://doi.org/10.3390/app14156705>

Academic Editor: Claudio Belvedere

Received: 28 June 2024

Revised: 29 July 2024

Accepted: 30 July 2024

Published: 1 August 2024



Copyright: © 2024 by the authors. Licensee MDPI, Basel, Switzerland. This article is an open access article distributed under the terms and conditions of the Creative Commons Attribution (CC BY) license (<https://creativecommons.org/licenses/by/4.0/>).

1. Introduction

Falls are the critical issue among vulnerable populations, including older adults, stroke survivors, Parkinson's patients, and individuals with other neurological disorders [1–7]. For example, up to one in three older adults falls at least once a year, while this figure is 40–58% for post-stroke individuals (within 1 year of their stroke) and 45–68% for people with Parkinsonism [8–14]. Due to slower reaction speeds and lower bone mineral density [15], these frail populations are prone to severe injuries that can lead to death or constant nursing care with large costs that can impact both individuals and national social security systems [15–17]. Falls prevention should be thus prioritized, especially for vulnerable populations. Among various causes, tripping has been detected as the leading cause,

accounting for more than half of the entire fall's incidences [18,19]. Prevention of tripping is thus of critical importance in reducing the overall incidence of fall-related injuries.

Tripping can be defined as the unintentional swing foot's contact with the walking surface or an object on it with sufficient momentum that destabilizes the walker. During the swing phase of the gait cycle, the critical event in relation to tripping risk is Minimum Foot Clearance (MFC), determined at the minimum swing toe height in the mid-swing phase [20,21]. Tripping at MFC has the high risk of forward balance loss and an associated fall due to the following factors: (i) low vertical clearance increases the likelihood of swing foot contact; (ii) swing foot travels at near-maximum speed, generating the large impact in the case of tripping at MFC; and (iii) both feet stance does not provide the ideal supporting base against balance loss [21–24]. MFC detection should ideally be based on the local minimum displacement; however, our previous study used maximum horizontal velocity for analyzing atypical MFC patterns.

Essentially, tripping prevention can be achieved if sufficient vertical displacement is provided at MFC [25]. There are various intervention techniques aiming to increase MFC height, such as use of the special shoe insole, biofeedback training, and exercise intervention. However, to our knowledge, there has been no intelligent device that predicts dangerous swing foot clearance and intervenes in real-time to increase MFC for tripping prevention. Therefore, the primary aim of this study is to develop and validate a machine learning model that predicts MFC heights in advance, facilitating its integration into assistive devices. The focus of our current research is, therefore, to predict MFC heights in advance so that this can be incorporated into assistive devices (e.g., active exoskeletons) for actuation assistance when necessary [26–29]. For development of such technology, MFC height estimation should be based on wearable sensors such as inertial measurement units (IMUs) [30–35] and undertaken well in advance for the mechanical device to take action in a relatively short timeframe. Our previous machine learning approach was first to show that MFC timing can be predicted based on toe-off kinematics with a small mean absolute error (i.e., 0.07 s) [36]. As the machine learning approach was effective for the temporal aspect of MFC (i.e., event detection and prediction), the aim of our research was to identify low MFC by applying a similar approach.

Recently, increased attention has been given to wearable sensors as practical gait assessment tools due to portability and practicality outside the laboratory environment. IMUs are among the most popular wearable sensors that have been utilized in biomechanical research [37]. Limited to the application in gait analysis, research efforts have been devoted into IMUs to become an alternative for optical motion capture systems and measure various gait data in everyday environments. IMUs application in this regard can be divided into event detection and spatial data measurement. Event detection has been attempted by redefining gold standard gait events only utilizing data obtained by IMUs such as linear accelerations and angular velocities in three dimensions. Prasanth et al. [37] provided a thorough review on gait event detection by IMUs, finding that heel contact and toe-off are the two major gait events on focus while other measures such as swing and stance phases can be determined secondary from the gait events. For example, heel contact accompanies foot contact impact that can be recorded by force plates, but IMUs measure accelerations that are affected by foot contact impact with the walking surface. Kim et al. [38] installed a single IMU inside the shoe insole to detect both heel contact and toe-off by characterizing particular acceleration patterns identified by time frequency analysis. MFC is more complicated to characterize its distinctive features because it takes place during the mid-swing phase without foot-ground interaction. MFC events can still be effectively detected by characterizing specific foot angles, maximum horizontal velocity (i.e., the transition to zero horizontal acceleration from a positive value), or zero vertical velocity at the lowest swing foot height (i.e., the transition to zero vertical acceleration from a negative value).

In addition to gait event detection, measurements of spatial data were undertaken by the application of IMUs. While temporal data can be highly associated with event detection

techniques, direct spatial data measurement requires completely different approaches. Double integration is one of the main principles to estimate spatial displacement. Despite proneness to errors due to 'drift', accelerations (m/s^2) can derive velocities (m/s) and then displacements (m). Köse et al. [39], for example, applied a single IMU on the pelvis to estimate step length with 2–3% errors, utilizing the Kalman filter in combination with double integration. In contrast to displacement estimation in the horizontal plane (i.e., step length), the previous study attempted the MFC height measurement by applying a regression model that incorporates fifteen features from IMUs [32]. Accurate measurement outside the laboratory environment is important, but if assistive devices are to be designed to increase MFC height in real-time to prevent tripping, 'predictability' is necessary. Instead of precise MFC height measurement, hazardous swing foot clearance should be classified in advance so that active actuation can take place in time to assist a wearer with providing further foot clearance to avoid tripping. It is, therefore, meaningful to take a classification approach instead of precise measurement for practical application.

The use of machine learning to study MFC height focuses mainly on predictive measurements. For example, Santhiranayagam et al. [40] used a generalized regression neural network (GRNN) to estimate MFC height using data from an IMU sensor. The GRNN-based MFC height predictions demonstrated a root mean square error (RMSE) of 6.6 mm with nine optimum features during treadmill walking. Miyake et al. [41] predicted minimum and maximum toe clearance height with radial basis function network (RBFN); accuracies in both cases still constituted a drawback. Instead, a recent idea was to study gait features by applying deep neural networks to heel contact and toe-off trajectories to predict other gait parameters [42]. Similar studies by Lee et al. [43] used deep convolution neural networks (DCNNs) to predict different types of gaits, which also precluded critical information on MFC heights. A classification of MFC height into categories is necessary to provide the required insight for technological intervention. The goal of this paper is to investigate the use of machine learning to classify MFC heights into categories so that a risky swing foot clearance, if determined in advance, will activate an actuator in time to assist a wearer. Thus, the required algorithm should be capable of quick computation for device actuation. In our current study, we have applied IMUs to record toe-off characteristics described by three-axial accelerations and angular velocities. The objective is to find out whether kinematics data following toe-off could be utilized for the classification of MFC heights into categories (e.g., high, medium, and low). Using the MFC characteristics in [20], the current study attempted to classify MFC into the following three sub-categories: (i) lower than normal ($MFC < 1.5$ cm), (ii) safe range (1.5 cm $<$ $MFC < 2$ cm), and (iii) well above the safety requirement ($MFC > 2$ cm). The outcomes of this research might help to predict risky (low MFC) swing foot clearance following the toe-off event utilizing a single IMU. The objective of the current study was to establish machine learning models to classify MFC data into different risk categories. Once a preliminary model is successfully developed, its prediction accuracy can be improved and generalized by feeding further data. Actuation to prevent tripping is an important consideration for active wearables such as exoskeletons and footwear. Development of such assistive devices could be an effective solution for minimizing tripping if such risks (low MFC) could be detected earlier in the swing phase, i.e., following toe-off.

Machine learning algorithms can extract and recognize features using mathematical relationships between different variables in the sample space [44]. A collection of mathematically related feature variables in a sample space forms the sample data for the development of training and testing algorithms. Machine learning applications in gait and neurological studies have created intrinsic understanding in previously underdiscovered areas, giving rise to wider applications involving neurological processes relating human gait from recognition of intention to physical locomotion [45–47]. In the current study, a range of supervised machine learning algorithms was used to build a classifier to make predictions on new unlabeled data points. The K-Nearest Neighbor (KNN) uses distance measures (e.g., Euclidean distance function) between every two data points to classify the points to

find the K-Nearest Neighbor. Random Forest and XGBoost use the decision tree ensemble for model representation and inference, but XGBoost uses a different training algorithm. XGBoost training is more complex than Random Forest because different computational kernels require specific optimization techniques. For example, XGBoost uses gradient boosting to train decision trees and focuses on minimizing the loss function, while Random Forest uses bagging to train decision trees and focuses on optimizing the hyperparameters in the parameter space. XGBoost is also a more complex and flexible model, which requires more parameter tuning, while Random Forest is simpler and more interpretable [48]. Since low MFC is associated with tripping falls [20], our work in this sense is to use machine learning algorithms to classify MFC heights into lower than normal, safe range, and above safe range categories. In addition to striving for accurate measurements as seen in other studies, our approach incorporates multiple classification layers to categorize tripping risks, therefore enhancing our ability to identify and mitigate them effectively.

2. Data Collection

2.1. Participants and Protocols

Six healthy young adults (age 23.5 ± 1.5 yrs.; height 172.0 ± 7.8 cm; body mass 79.5 ± 15.5 kg) were recruited for the current research from the university volunteers. To be included in this study, participants were required to be healthy, capable of walking on the treadmill for 30 min without a break, free from injuries that affect their walking patterns, and have no previous history of injurious falls for at least the past two years. The entire experimental protocol was explained by the researchers, and an informed consent form approved and mandated by the Victoria University Research Ethics Committee was voluntarily signed by the participants prior to participation.

Gait testing was conducted on the treadmill (AMTI) for 5 min at 4 km/h, which was considered to be the reasonable preferred pace for healthy young individuals [49]. The Vicon Bonita system (Nexus 2.12.1) with 10 cameras was utilized to track reflective markers at 200 Hz, attached to the heel (the proximal end of the shoe) and the toe (the most anterior superior surface of the shoe). Utilising the analytic software (i.e., Visual 3D, C-motion, Oakville, ON, Canada, <https://c-motion.com/>), a low-pass Butterworth filter (6 Hz) was applied to the obtained position data prior to analysis. Based on the kinematic conventions [50], toe-off and heel contact were first computed to define the swing phase. MFC was identified as the local minimum height of the toe during the mid-swing phase, but when the clear local minimum was absent, the alternative definition was applied utilizing the maximum horizontal velocity of the swing toe [51].

As illustrated in Figure 1, IMU (Nexus, Trident) was attached to the mid-foot section to record various foot-segment-based kinematic data (200 Hz), but for the current study, tri-axial linear accelerations (AccX, AccY, and AccZ) and angular velocities (GyroX, GyroY, and GyroZ) were obtained for machine learning applications. The overall goal of this study was to predict in which category (Table 1) upcoming MFC would be classified based on the five consecutive frames from toe-off comprising 0.025 s kinematic information from toe-off. In other words, algorithms were developed for a single Inertial Measurement Unit (IMU) (see Figure 1) to predict the upcoming MFC height category, as established by the 3D motion capture system. MFC categories employed in the current study are described in Table 1, determined by the previous studies indicating the average MFC for young adults to be about 1.5 cm (R1), slightly above the average up to 2 cm (R2), and minimum risk of tripping (R3) as above 2 cm [20,21,52].



Figure 1. IMU (Nexus, Trident) attached to the mid-foot; tri-axial linear accelerations and angular velocities are indicated by arrows. X is the anterior–posterior axis, Y is the medio-lateral axis, and Z is the vertical axis.

Table 1. MFC categories describing the three subclasses (R1, R2, and R3) or targets for ML training.

R1	R2	R3
Below average	Safe	Well-above safety limit
MFC < 1.5 cm	1.5 cm < MFC < 2 cm	MFC > 2.0 cm

2.2. Data Exploration

The selected features (i.e., tri-axial linear accelerations, angular velocities) were plotted with a Seaborn pair plot [53] and showed non-linearly separable classes. The average values are indicated in Table 2.

Table 2. Data from the IMU sensor showing mean and standard deviation (five frames from toe-off; 0.025 s) of feature variables and number of counts per category of the 18,490 datasets collected. STD = standard deviation; Acc = linear acceleration; Gyro = angular velocity; x, y, z = three dimensions and rotational axes.

Category		Average Value of Corresponding Feature Variables						Total
		AccX (m/s ²)	AccY (m/s ²)	AccZ (m/s ²)	GyroX (rad/s)	GyroY (rad/s)	GyroZ (rad/s)	
R1	Mean	10.54	−3.85	4.18	0.02	−1.64	0.55	7235
	STD	5.92	5.81	4.79	2.75	1.91	2.11	
R2	Mean	9.89	−2.00	0.16	0.09	−0.69	0.10	3738
	STD	4.40	5.34	4.08	1.51	1.12	1.84	
R3	Mean	8.43	−0.23	8.09	2.34	−3.22	1.83	7517
	STD	7.06	3.94	7.28	2.00	2.10	2.01	

The zoomed Z-axis component of the acceleration and angular velocity on the three categories of the MFC heights shows distinctive patterns illustrated in Figure 2a,b, and argues the range of our classification.

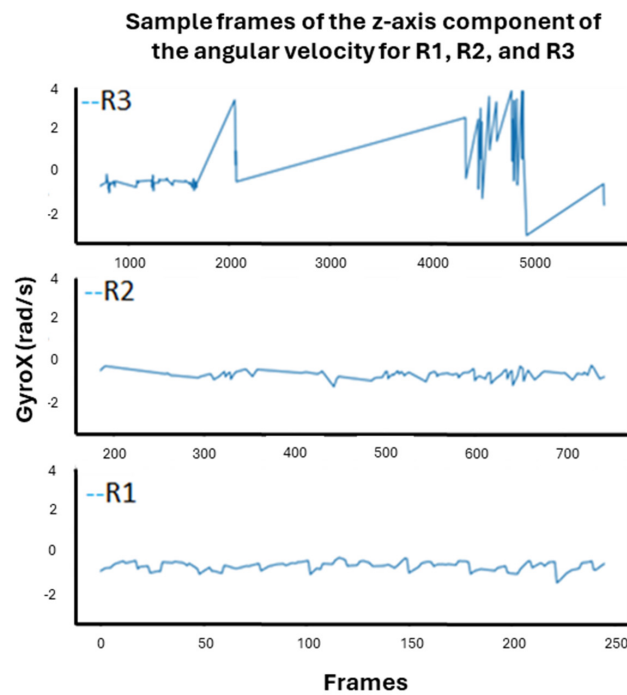
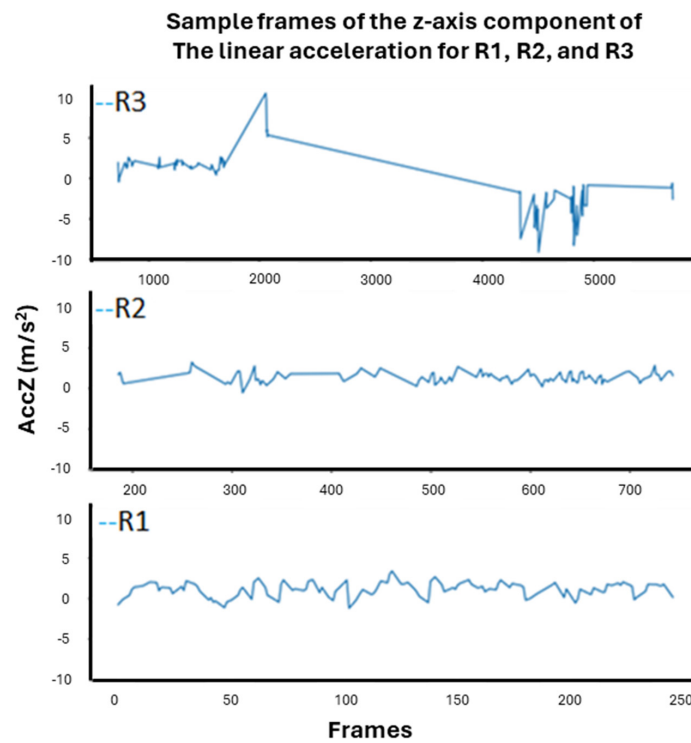


Figure 2. (a) Zoomed Z-axis of linear acceleration on the target sets R1, R2, and R3 graphically compared. The graph represents tri-axial frames of the acceleration on the Z-axis for all tagged targets of our MFC categories. (b) Zoomed Z-axis of angular velocity on R1, R2, and R3 graphically compared. The graph shows the characteristic tri-axial angular acceleration frames on the three MFC height categories.

2.3. Model Selection and Algorithm Design

As shown in Figure 3, the dataset features are non-linearly separable, and characteristic attributes of each data point form a category that is assigned to a class. To address this classification task, this study used K-Nearest Neighbor (KNN), Random Forest, and XGBoost supervised machine learning methods.

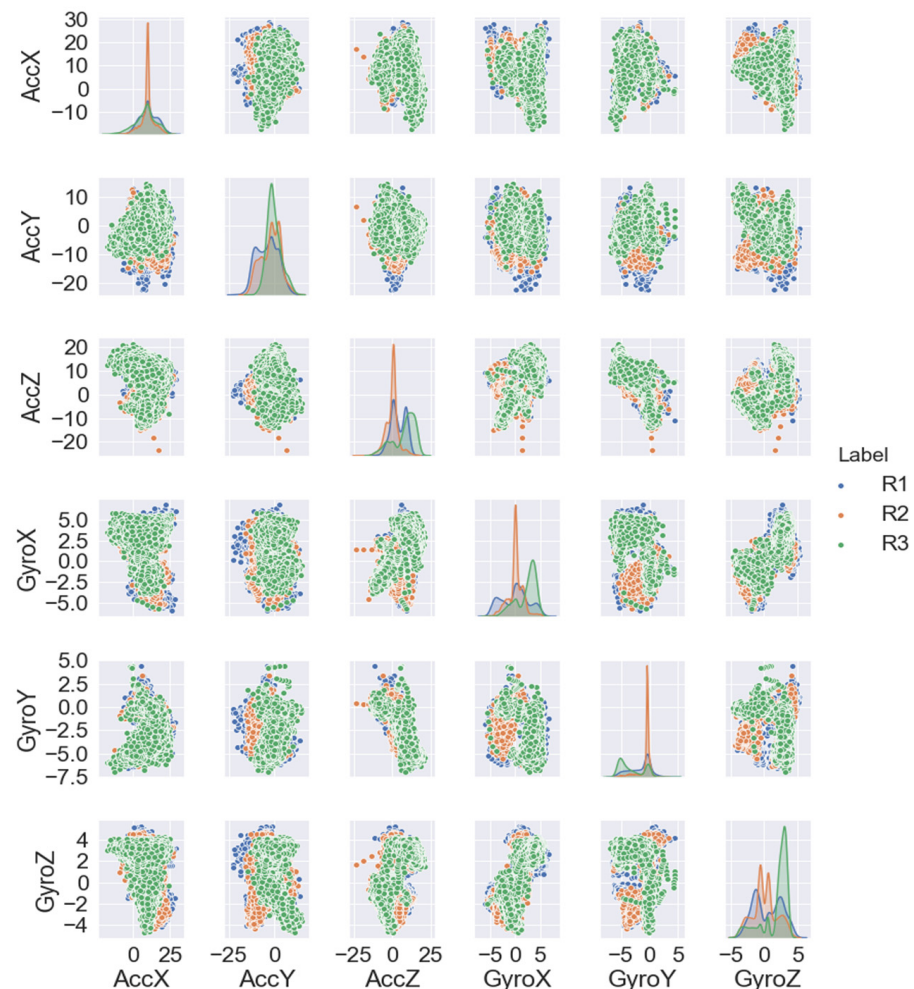


Figure 3. Pair plot correlation of the feature variables (linear acceleration and angular velocity) on the target R1 (blue), R2 (orange), and R3 (green). Acc = linear acceleration; Gyro = angular velocity; x, y, z = three dimensions and rotational axes.

These methods have proven success in several use cases in gait classification and identification [54,55]. Additionally, given the focus of this study, all three methods were sourced from prior studies, where these algorithms were used with IMU-sourced data, particularly using KNN (e.g., [56,57]), Random Forest (e.g., [58]), and XGBoost (e.g., [59]). The choice of classification approaches was supported by [60], where KNN and RF were identified among the top-performing algorithms for classification of human motion data using IMUs. Further consideration of the selection was the characteristics of the data used in this study, namely assumptions about data distribution, robustness to non-linear relationships, and the potential to leverage multiple algorithms and yield better performance while maintaining some interpretability with further applications [61]. The selection of these classical machine learning algorithms also allowed benchmarking with similar studies, where Random Forest and boosting approaches (such as XGBoost) were shown to achieve higher classification accuracy in similar settings [58,59].

Using KNN, Random Forest, and XGBoost allowed us to leverage the stronger points of each of the algorithms. Compared to Random Forest and XGBoost, K-Nearest Neighbor (KNN) uses distance measures (e.g., Euclidean distance function) between every two data points to classify the points to find K-Nearest Neighbor. Given the relatively small number of features in the model, training time for KNN was not a concern, while XGBoost was expected to perform well with low-variance features. Comparing the performance of KNN to Random Forest and XGBoost would allow us to avoid overfitting concerns as well as leverage KNN results for their interpretability.

KNN is one of the main supervised learning algorithms with a relatively simple structure that can be used in both classification and regression tasks. In KNN, each instance is categorized as a vector of numbers in an n -dimensional Euclidean space. To find the class to which an unknown data point is a neighbor, the Euclidean distance was measured. All instances, therefore, correspond to points in an n -dimensional Euclidean space, and the distance between instances $d(p,q)$ is as follows:

$$\begin{aligned} d(p,q) &= \sqrt{(q_1 - p_1)^2 + (q_2 - p_2)^2 + \dots + (q_n - p_n)^2} \\ &= \sqrt{\sum_{i=1}^n (q_i - p_i)^2} \end{aligned}$$

Given K-Nearest Neighbor, the optimum value is picked for the best prediction of either the R1, R2, or R3 MFC height category.

On the other hand, Random Forest and XGBoost algorithms offer a different approach by using ensemble learning for supervised machine learning tasks.

In Random Forest, an ensemble of many decision trees is designed to overcome overfitting problems associated with decision trees by bootstrap aggregation or bagging. Given a Random Forest tree T_b (for $b = 1$ to B) to the bootstrap sample Z^* of size N from training data, a prediction at a new point x is made using the following classification:

$$\hat{C}_{rf}^B(x) = \text{majority vote } \{\hat{C}_b(x)\}_1^B$$

where

$\hat{C}_b(x)$ is the class of prediction of the b th Random Forest.

This study used the Gini impurity as a measure to quantify the purity of a node in a decision tree. This study used tuning to test the number of trees, the minimum number of data points in a node that were required for the node to be split further, and the number of predictors that was randomly sampled at each split when creating the tree models.

Compared to Random Forest, XGBoost uses gradient boosting with regularization, i.e., the algorithm uses decision tree ensemble but optimizes performance by redefining boosting with the objective to minimize losses by adding weak learners using gradient descent [48]. The results of testing with KNN, Random Forest, and XGBoost are presented and analyzed (e.g., Table 3).

Table 3. Performance summary of KNN, Random Forest, and XGBoost.

Algorithm	Accuracy Score (%)	Weighted Average (%)	Model Training Time
KNN	84	83	0.39 s at K = 12
Random Forest	86	86	13.98 s, 800 estimators, and max depth = 8
XGBoost	75	74	170.98 s (n_estimators = 2, max_depth = 2, learning_rate = 1, objective = 'multi: softprob', num_round = 25)

Data Splitting, Hyperparameter Tuning, and Optimizing

At the initial stage, the data were split, with 70% allocated for testing and 30% for training. The stratified splitting technique was applied to ensure the same frequency distribution of the outcome in the analysis and assessment sets. Cross-validation was implemented with 5k folds and later confirmed with 10k folds and 5 repeats, where the data were split into 10 parts with different random shuffles of the data each time. Since every part is used as the test set only once, this provides more stable and reliable estimates of model performance because it averages the results over more splits/shuffles of the data. Additionally, this approach was used to provide a better bias–variance trade-off. Input variables were normalized (Table 2) using RobustScaler. Using this approach, the data were transformed by removing the median and scaling according to the quantile range (i.e., between the 25th and 75th quantiles). Such an approach ensured robustness to outliers and non-reliance on distributional assumptions, which were particularly important for employed ML algorithms (e.g., KNN).

GridSearch cross-validation was used to determine the optimal list of parameters for machine learning models. The overfitting concerns were addressed by repeating the grid search via racing with ANOVA models [62]. Such racing methods in combination with parallel processing have shown faster performance compared to sequential grid search approaches. Fitting 5 folds and iterating for 28 candidates, totaling 140 fits, the best parameters for KNN were tested with 7 neighbors, 2 distances, 2 weights, and 5 cross-validations, and the best parameters proposed were (`{'n_neighbors': 13, 'p': 2, 'weights': 'distance'}`). Similarly, Random Forest's best parameter suggestion with GridSearch was (`{'criterion': 'gini', 'max_depth': 8, 'max_features': 'sqrt', 'n_estimators': 400, 'random_state': 42}`).

Feature importance using permutation analysis was completed for the developed models and presented graphically. The importance of a feature was measured by calculating the increase in the model's prediction error after permuting the feature. The importance was defined if the shuffling feature's values increased the model error [63].

The feature variables (accelerometer and angular velocity) were separately investigated to determine individual contributions to the prediction of the MFC heights. The results are shown in Table 4a,b.

Table 4. (a) Comparison of prediction accuracies using linear acceleration and angular velocity as separate features on KNN, Random Forest, and XGBoost. (b) Comparison of individual axial features (acceleration and angular velocity) on prediction with KNN, Random Forest, and XGBoost.

(a)						
Training Features	KNN (% Accuracy)	Random Forest (% Accuracy)	XGBoost (% Accuracy)			
Acceleration (X, Y, Z)	65	67	60			
Gyro meter (X, Y, Z)	74	75	64			
Combined Acceleration and Gyro meter (X, Y, Z)	84	86	75			
(b)						
ML Algorithm	Percentage Accuracies of Individual Features for Predicting MFC Height					
	AccX (%)	AccY (%)	AccZ (%)	GyroX (%)	GyroY (%)	GyroZ (%)
KNN	41	45	55	56	51	55
Random Forest	40	43	51	51	46	48
XGBoost	46	53	56	58	56	60

3. Results

Figure 2a,b depict a clear difference on the Z-axis variables of the critical MFC heights. MFC height in the range of the critical threshold based on the young population's lower end of the normal range (i.e., mean $-$ SD) indicated the Z-axis component of the kinematic variable is highly unstable with increased tripping risk. Figure 3 is the correlation plot that helped us visualize the relationship between the variables and the target.

This study followed best practices and employed a range of classical performance metrics for classification, including confusion matrix, classification accuracy, precision, recall, F1-score, and the ROC AUC [64]. A combination of the metrics was used where high accuracy referred to the model's high level of overall correctness, with high recall showing the proportion of actual positive cases and precision indicating the proportion of positive identifications made by the model that were actually correct. The F1-score is used to show the balance of precision and recall, and the ROC AUC score shows the ability of the model to discriminate between classes.

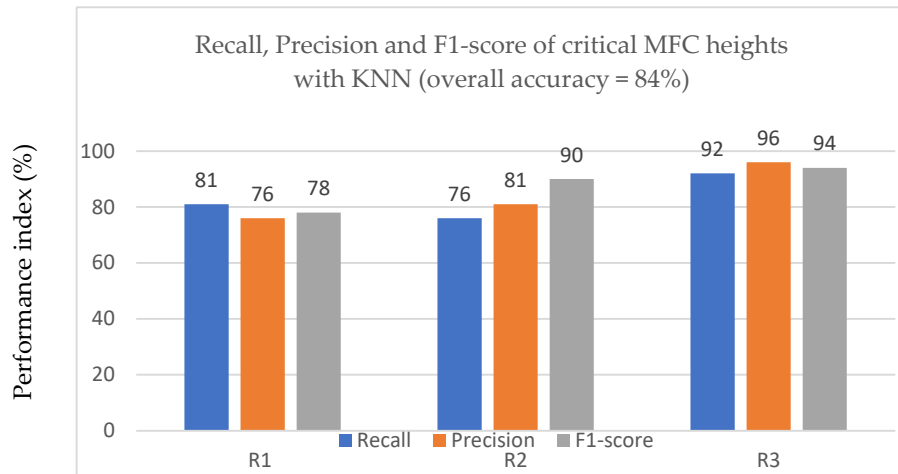
Figure 4a–c represent the classification results derived from the confusion matrix for KNN, Random Forest, and XGBoost with close-matched accuracies in KNN and Random Forest. Higher accuracies are prioritized in ML modeling, while precision and recall rate gave further insight on the overall performance of the model. For example, high recall signifies good coverage, i.e., the percentage of positive tags the classifier predicted correctly out of all the positive tags available in the sample, while precision is indicative of the proportion of actually positive classes out of all the classes predicted as positive [65]. The F1-score measures recall and precision at the same time using harmonic means. It implies the model's balanced ability to both capture true positive cases (recall) and be accurate with the cases it does capture (precision). Both precision and recall are represented in the three categories supported by the F1-scores. In the KNN model, a particular MFC height is predictable with 84 percent accuracy. Recall and precision are 92 and 96 percent, respectively, on R3 (when MFC heights are above safety limits). At the same time, the F1-score on R3 is 94 percent but decreased in the R1 and R2 categories. Similarly, in the Random Forest model, recall, precision, and F1-scores have the same value at above safety regions (R3) with an overall model performance of 86 percent. Random Forest was more sensitive than KNN and XGBoost at lower MFC height categories. At best, XGBoost has an average performance of 75 percent throughout. Like KNN and Random Forest, XGBoost optimal prediction was above safety limits (R3) and performed the least at below safety (R1) and safety categories (R2). XGBoost had a nearly 50–50 chance of predicting positive cases of safety MFC heights with an F1-score of 56 percent and 10 percent higher when the MFC height is below average. These are regions which measure very low MFC heights. The model training time for KNN was much quicker at 0.39 s compared to 13.98 s with Random Forest and 170.98 s with XGBoost, as shown in Table 3.

The bar chart shows that the KNN parameters developed in this model are good at predicting positive cases of MFC height that are well above the safety limit. It performed better in accurately classifying MFC heights at the safety and well-above safety limits than when MFC height is below average.

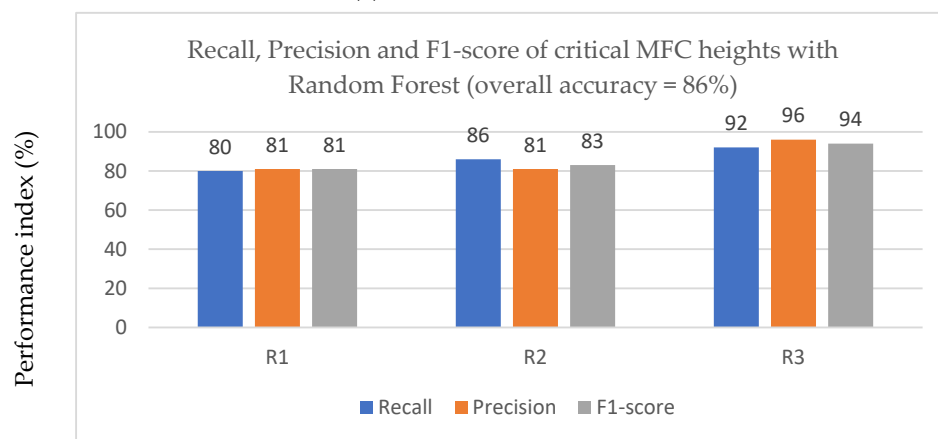
There is a near-equitable distribution of the metric with an overall accuracy of 86%. Recall and precision of MFC heights below average (R1) are lower than observed at safety and well-above safety MFC heights. Precision, recall, and F1-score of Random Forest and KNN have similar performance indexes in well-above safety regions.

In summary, the performance result with Random Forest is similar to the KNN algorithm, with a slight improvement in overall accuracy and recall and a higher training time. Random Forest randomly selects a subset of features that are used as candidates at each split. This protocol automatically prevents the multitude of decision trees from relying on the same set of features, solving problems of overestimated correlations by avoiding a correlation of the individual trees. Each tree then draws a random sample of data from the training dataset when generating its splits, which further introduces an element of randomness and prevents the individual trees from overfitting the data. The uniformly

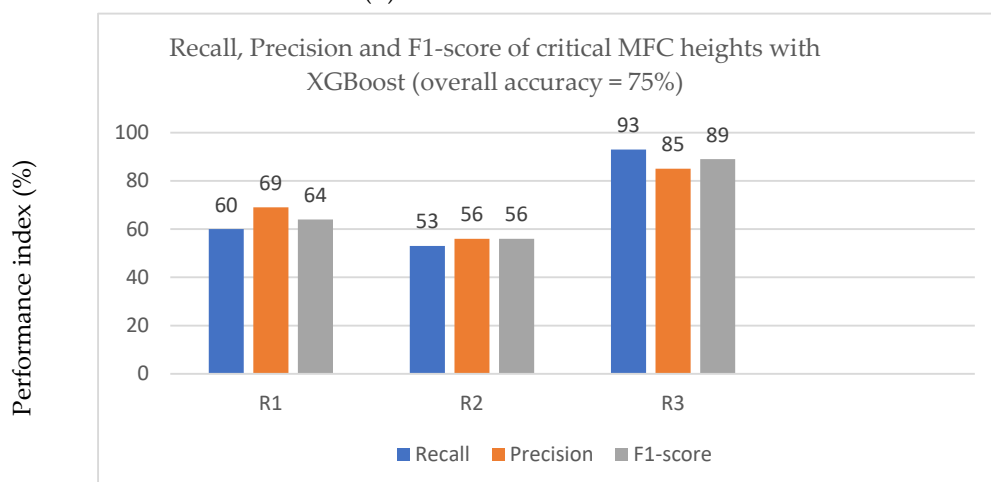
generated weighted average on R1, R2, and R3 with both algorithms showed that each class was equally considered in its calculation of the metrics and had equal impact on the average score for each of those metrics (Table 3).



(a)



(b)



(c)

Figure 4. Cont.

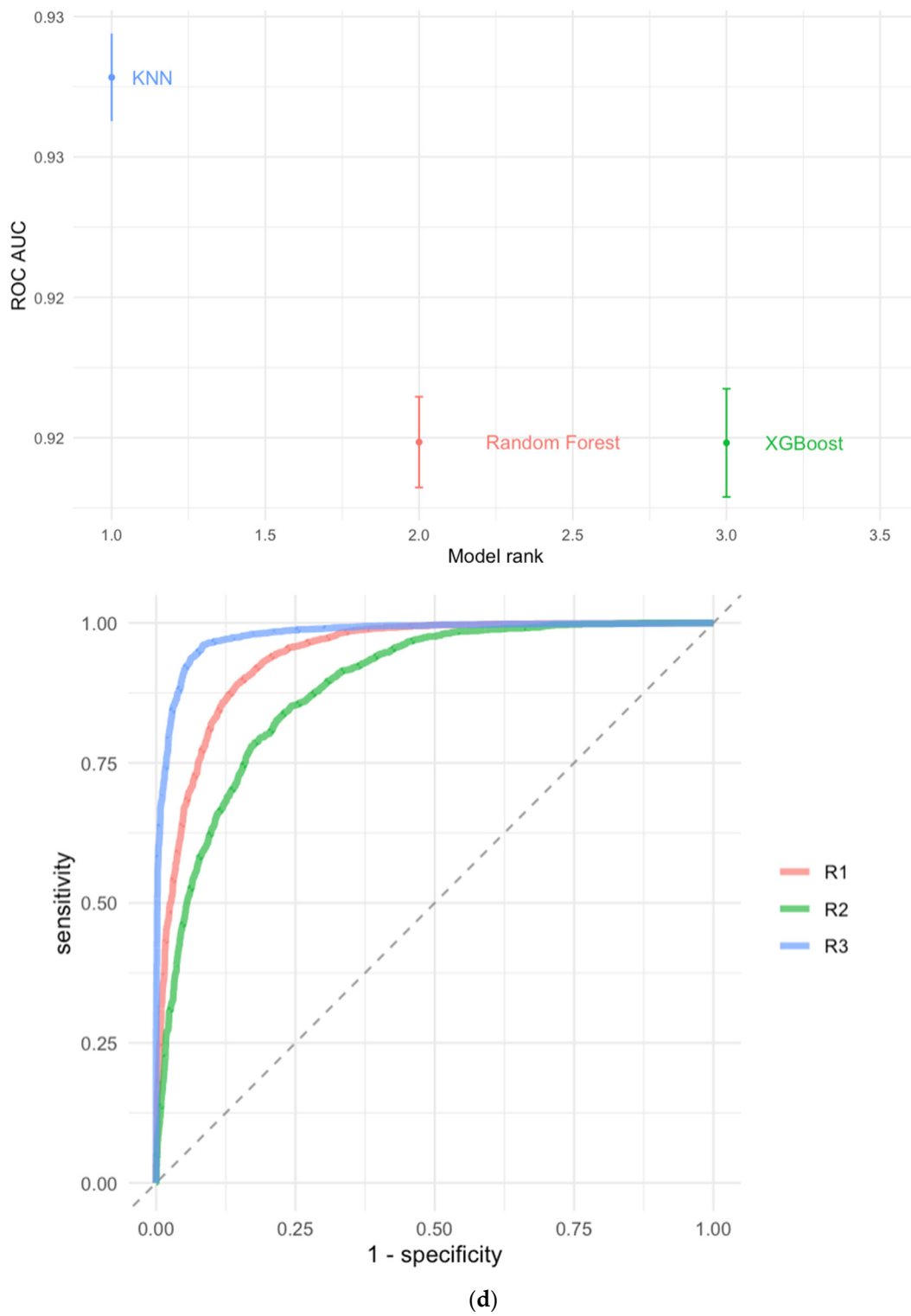
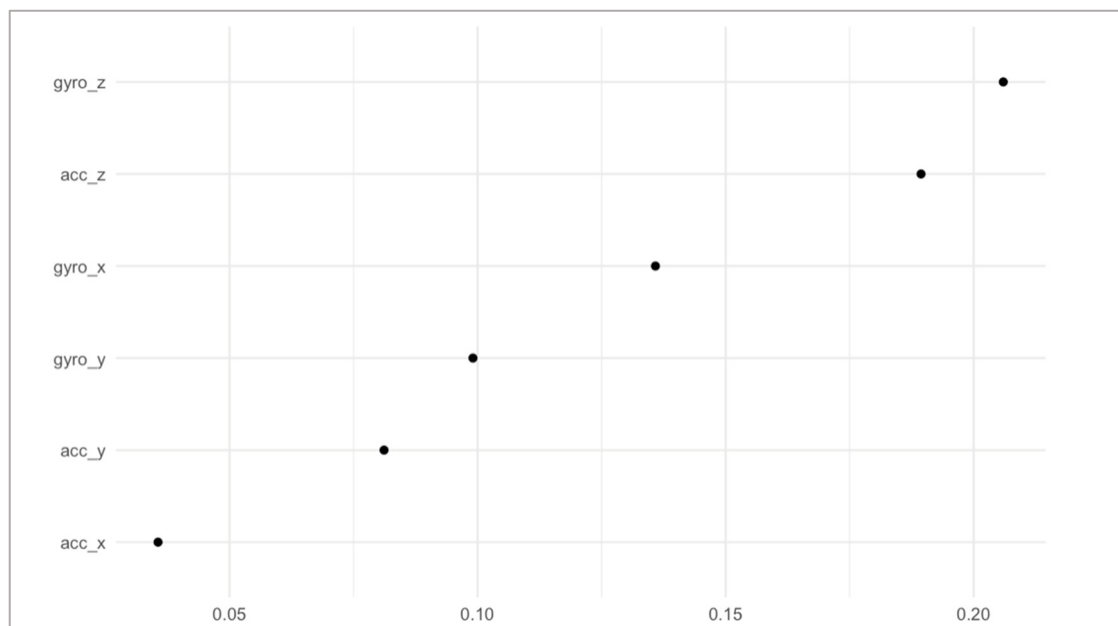


Figure 4. Cont.



(e)

Figure 4. (a) Performance evaluation of the KNN algorithm showing average accuracy of 84 percent with high recall and F1-scores. (b) Performance evaluation of Random Forest with average accuracy of 86 percent with high recall and F1-scores. (c) Performance evaluation of XGBoost stands at 75% accuracy in classifying MFC heights into the following three pre-defined categories: below average, safety, and well-above safety limits. The recall, precision, and F1-score index at well-above safety limits are below that observed with Random Forest and KNN. XGBoost can detect positive cases at well-above safety limits with a greater chance of error than observed in other models. (d) Comparison of model performances based on ROC AUC where higher values indicate a better separability, which is higher discrimination capacity to distinguish between classes and further comparison for discrimination capacity between each class. (e) Feature importance evaluation in classing MFC heights into the following three pre-defined categories: below average, safety, and well-above safety limits.

Table 3 shows the comparison between prediction accuracy and model training time on KNN, Random Forest, and XGBoost. XGBoost has the lowest accuracy and highest training. KNN has the quickest training time and closely follows Random Forest in accuracy.

A comparison of the ROC AUC scores is presented in Figure 4d, where all three algorithms show high discrimination capacity, with KNN outperforming the rest (consistent with the prior results).

Further assessment was performed on feature importance as presented in Figure 4e.

The results of the algorithm showed that the three most important features for the classification were measurements from angular velocity Z (Gyro_Z) and linear acceleration Z (Acc_Z). This confirmed the initial results that the increased tripping risk is associated with the Z-axis components.

We further examined the prediction accuracies of the separate linear accelerations and angular velocities together and as individual features contributing to the MFC heights. The results are shown in Table 4a,b. The feature importance assessment was conducted using the 'sklearn' package and is shown graphically.

It was observed that the combined linear acceleration and angular velocity features had a more positive impact on the overall performance accuracies of the three models. However, individual features contributing to the prediction varied. Table 4b showed that the Z-axis component of the linear acceleration and the X-axis and Y-axis components of the angular velocity had greater influence on the MFC heights than the other kinematic features used for the training.

Table 4a shows the angular velocity had a more positive effect on the predicted MFC heights than the linear acceleration, and MFC height is best predicted with multiple features. Table 4b indicated that the vertical acceleration and the X and Z axes of the angular velocities are more significantly related to the MFC height than the other kinematic variables ($p < 0.001$).

The ROC AUC scores show how well the model performs with no knowledge of the class imbalance and take values from 0–1. Table 5 shows the AUC scores on all three models in each target class. The scores are represented by both high recall and high precision, where high precision relates to a low false positive rate and high recall relates to a low false negative rate. The high scores for both show that the classifier returns accurate results (high precision), as well as a majority of all positive results (high recall). Again, KNN and Random Forest had higher AUC scores than XGBoost.

Table 5. The macro average area under curve (AUC) score for each target class (R1, R2, and R3) on different machine learning models.

	Random Forest	KNN	XGBoost
R1	0.87	0.84	0.73
R2	0.83	0.71	0.73
R3	0.97	0.92	0.89

The high AUC score across each model indicates that none of the model's performance is a random prediction. KNN and Random Forest are the best-performing models to correctly classify the three MFC categories. To operationalize the model, a quick computation time becomes a leverage when the AUC scores are closely matched, and the computational time has considerable impact as a preferred margin to increase effectiveness.

4. Discussion

Minimization of tripping risks has been one of the central issues for fall prevention, and providing sufficient swing foot–ground clearance at MFC has been a key consideration while applying an intervention. For the real-time technology as part of the intelligent system, one effective approach is to use feed-forward prediction of upcoming MFC as early as the initiation of the swing phase at toe-off. For healthy young adults, MFC usually takes place approximately around 50% of the swing phase, 0.2 s–0.3 s after toe-off [66]. It can be interpreted that ‘prediction and actuation’ should, in this example, occur within the mentioned time limit. In the current study, KNN successfully classified MFC into the three categories at 84% accuracy within 0.025 s, suggesting the sufficient reliability and feasibility of our machine learning outputs to be incorporated into intelligent assistive devices. Previous methods for MFC height estimation based on double-integration of vertical acceleration [22] are useful for taking measurements outside the laboratory environment; however, our machine learning-based prediction is the first attempt to devise intelligent active exoskeletons to increase MFC height. We have previously demonstrated that toe-off kinematics can be used to predict MFC timing [36]; in this research we have applied toe-off kinematics for the real-time feedforward prediction of MFC heights.

Machine learning approaches are the emerging technique for classification and evaluation of gait patterns based on large data volumes, considered to be the mainstream analytical method in the future and replacing conventional, complex, manual, and customized mathematical programming. The prediction of a future gait event can be incorporated into assistive devices for them to become intelligent real-time systems for augmenting human ambulation. In machine learning use cases, we have employed KNN, Random Forest, and XGBoost for gait classification. All the models successfully classified MFC height into the three subcategories from toe-off information at high accuracies except for XGBoost. Nevertheless, caution is required for machine learning algorithms to provide feedforward control for a powered assistive device in a timely manner. While Random Forest showed better

performance in accuracy, KNN may be the preferred option considering the time taken for prediction to activate assistive devices at MFC based on a preceding toe-off event. High recall and high precision cannot be compromised to ensure correct classification of MFC heights for the populations at critically high and moderate tripping risks, respectively [65]. Further collection of the data is essential in feeding the developed algorithms to improve performance before equipping them into assistive devices for people. It is, however, the primary advantage of the machine learning approach, meaning that the prediction accuracy can basically only improve as data feeding progresses. Our research can be a groundwork for further development for practical equipping with lower limb active exoskeletons.

In addition to the essential data feeding, there are some other fundamental concerns to overcome for practical application into assistive devices as intelligent systems. In the current proof-of-concept research, data of healthy young participants were selected to build the algorithms, but prediction of the tripping risk is more useful for vulnerable populations such as older adults, stroke survivors, people with Parkinson's disease, and other pathological conditions. Gait patterns of the high-tripping-risk group are often clearly different from the healthy young group, implying that the currently developed algorithms require fine-tuning for each gait pathology. MFC classification requires reconsideration, i.e., the further sub-divisions of the lower end (e.g., less than 0.5 cm, 1 cm, etc.) should be tested to examine the hazardous risk rather than the MFC below 1.5 cm categorization. Such risk detection can be useful not only for frail, pathological older adults but also for younger individuals in cases of physical inactivity or when operating in visually restricted environments, such as the sport industry.

After data feeding from various populations is carried out to achieve certain reliability in recognizing hazardous MFC heights, the developed intelligent systems can be incorporated into ankle active exoskeleton devices to directly control ankle motion in order to increase MFC and prevent the risk of tripping falls. Kubota et al. [67] introduced the active ankle exoskeleton based on hybrid assistive limb (HAL) technology, which operates ankle dorsiflexion–plantarflexion motion based on efferent neural signals. In another word, HAL technology utilizes intention to make movements to precisely control exoskeletons and reproduce intended movements, known to enhance motor control functions and improve neurological disorders [68,69]. Ankle-HAL technology was developed for rehabilitation to focus on joint motion training by users' own neuro-signals, therefore not designed to directly assist active walking [51,70]. Incorporation of the ML algorithm and feedforward actuation to reduce the tripping risk could be possible by operating the exoskeletons with kinematic inputs. This approach represents a promising direction for tripping risk mitigation. Unlike traditional methods that may rely solely on the user's bio-electrical signals—which can be unreliable in populations at high risk of falls—actuation in this model can be dynamically managed based on external conditions. This proactive intervention method directly reduces tripping risks by integrating real-time user-specific movement patterns into the decision-making process of assistive devices. If ankle control is not based on neuro-signals, rehabilitation effects on motor control may be lower, but in return, wearers can be expected to learn the optimum ankle motion during the swing phase and acquire less trip-prone walking patterns. Such application is one of the more prospective directions of the current research outcomes for practical rehabilitation settings, while continuous research efforts are essentially required.

Although further consideration may be required before practical application, IMU attachment to the mid-foot section as illustrated in Figure 1 can be incorporated into the ankle active exoskeleton. If the ankle exoskeleton is to be worn to directly assist walking, the size of the motor actuator should be minimized while providing sufficient torque for supporting dorsiflexion and increasing MFC. Combined with our previous attempt to identify MFC timing from toe-off kinematics [38], the current findings represent the groundwork for prototyping the intelligent prediction system, which is utilized to reduce tripping risk. Motor actuation torque and its effects on MFC should be tested, as only 1° of ankle dorsiflexion is estimated to increase toe height by more than 0.3 cm [26]. Therefore,

no exaggerated ankle motion is required. Battery requirement is another consideration, but may not be a critical limitation if only subtle effects are demanded to prevent tripping, which can avoid triggering any negative side effects on other gait patterns.

As highlighted throughout the discussion, this study acknowledges several limitations that warrant attention in future research. Firstly, the sample size and diversity need expansion. The testing algorithms on healthy young adults provided a foundational model and a total of 18,490 swing phase gait cycles. Data were extracted from six healthy young adults, extending the application to populations prone to tripping, such as older adults or those with motor impairments. Additionally, the classification was restricted to three categories; introducing more nuanced categories could enhance the precision of tripping risk predictions without compromising measurement accuracy. Advances in data collection will facilitate these improvements. Moreover, integrating deep learning techniques could refine the accuracy of tripping risk predictions. For practical applications, especially in active exoskeletons, achieving early predictions with minimal computation time remains a priority in addition to accuracy. Incorporating efferent bioelectrical signals could further enhance the predictability of risky swing toe clearances. Optimization efforts should also explore positional data through double-integration of acceleration signals and the use of pressure sensors to acquire kinetic and foot center pressure data. Subjective feedback on comfort, usefulness, and everyday feasibility must also be optimized for practical use.

5. Conclusions

Tri-axial linear accelerations and angular velocities data from a single IMU sensor mounted on the mid-foot effectively classified Minimum Foot Clearance (MFC) into the following three categories: (i) less than 1.5 cm, (ii) 1.5–2.0 cm, and (iii) more than 2.0 cm. However, as the data were collected from only six healthy young adults, this study's limitations include a need for a broader dataset encompassing more diverse population groups. Future research should target individuals at higher risk of tripping-related falls, such as older adults, stroke survivors, and individuals with neurological disorders, including Parkinson's disease and dementia.

In conclusion, this study has confirmed the potential of using machine learning, specifically KNN, to predict MFC heights with a high degree of accuracy (84%) and efficiency. While the initial results are promising, the performance of MFC prediction needs further validation using different machine learning algorithms and a wider range of populations. This research supports the application of such predictive models in the control systems of movement assistive devices. Future studies should consider employing advanced machine learning techniques, such as convolutional neural networks (CNNs), transformers, and ensemble models, to improve predictive accuracy. Additionally, expanding the dataset size is crucial. The analysis also revealed that vertical acceleration and the 'x' and 'z' components of angular velocities are primarily associated with Minimum Foot Clearance height.

Author Contributions: Conceptualization, H.N. and R.B.; methodology, H.N., C.O.A. and R.B.; software, M.P. and C.O.A.; validation, M.P. and C.O.A.; formal analysis, C.O.A.; investigation, H.N., M.P., C.O.A. and E.S.; writing—original draft preparation, H.N. and E.S., writing—review and editing, H.N., M.P. and R.B.; supervision, R.B. All authors have read and agreed to the published version of the manuscript.

Funding: This research was funded by the VESKI—Study Melbourne Research Partnerships (SMRPs) program, grant number VESKI-SMRP #2003, and the Australian Research Council (ARC) DP200103583.

Institutional Review Board Statement: This study was conducted in accordance with the Declaration of Helsinki and approved by the Ethics Committee of Victoria University (HRE23-017, approved on 30 June 2023).

Informed Consent Statement: Informed consents were obtained from all subjects involved in this study.

Data Availability Statement: The raw data supporting the conclusions of this article will be made available by the authors on request.

Acknowledgments: We extend our deepest gratitude to Yoshiyuki Sankai, CYBERDYNE Inc., for his invaluable guidance and support throughout this project.

Conflicts of Interest: The authors declare no conflicts of interest.

References

1. Srivastava, S.; Muhammad, T. Prevalence and risk factors of fall-related injury among older adults in India: Evidence from a cross-sectional observational study. *BMC Public Health* **2022**, *22*, 550. [[CrossRef](#)] [[PubMed](#)]
2. Prudham, D.; Evans, J.G. Factors associated with falls in the elderly: A community study. *Age Ageing* **1981**, *10*, 141–146. [[CrossRef](#)] [[PubMed](#)]
3. Tinetti, M.E.; Speechley, M.; Ginter, S.F. Risk factors for falls among elderly persons living in the community. *N. Engl. J. Med.* **1988**, *319*, 1701–1707. [[CrossRef](#)] [[PubMed](#)]
4. Wei, W.E.; De Silva, D.A.; Chang, H.M.; Yao, J.; Matchar, D.B.; Young, S.H.Y.; See, S.J.; Lim, G.H.; Wong, T.H.; Venketasubramanian, N. Post-stroke patients with moderate function have the greatest risk of falls: A national cohort study. *BMC Geriatr.* **2019**, *19*, 373. [[CrossRef](#)] [[PubMed](#)]
5. Fasano, A.; Canning, C.G.; Hausdorff, J.M.; Lord, S.; Rochester, L. Falls in Parkinson’s disease: A complex and evolving picture. *Mov. Disord.* **2017**, *32*, 1524–1536. [[CrossRef](#)] [[PubMed](#)]
6. Pressley, J.C.; Louis, E.D.; Tang, M.X.; Cote, L.; Cohen, P.D.; Glied, S.; Mayeux, R. The impact of comorbid disease and injuries on resource use and expenditures in parkinsonism. *Neurology* **2003**, *60*, 87–93. [[CrossRef](#)] [[PubMed](#)]
7. Cattaneo, D.; Gervasoni, E.; Pupillo, E.; Bianchi, E.; Aprile, I.; Imbimbo, I.; Russo, R.; Cruciani, A.; Turolla, A.; Jonsdottir, J.; et al. Educational and Exercise Intervention to Prevent Falls and Improve Participation in Subjects With Neurological Conditions: The NEUROFALL Randomized Controlled Trial. *Front. Neurol.* **2019**, *10*, 865. [[CrossRef](#)] [[PubMed](#)]
8. Hornbrook, M.C.; Stevens, V.J.; Wingfield, D.J.; Hollis, J.F.; Greenlick, M.R.; Ory, M.G. Preventing falls among community-dwelling older persons: Results from a randomized trial. *Gerontologist* **1994**, *34*, 16–23. [[CrossRef](#)] [[PubMed](#)]
9. Hausdorff, J.M.; Rios, D.A.; Edelberg, H.K. Gait variability and fall risk in community-living older adults: A 1-year prospective study. *Arch. Phys. Med. Rehabil.* **2001**, *82*, 1050–1056. [[CrossRef](#)]
10. Alemdaroğlu, E.; Uçan, H.; Topçuoğlu, A.M.; Sivas, F. In-hospital predictors of falls in community-dwelling individuals after stroke in the first 6 months after a baseline evaluation: A prospective cohort study. *Arch. Phys. Med. Rehabil.* **2012**, *93*, 2244–2250. [[CrossRef](#)]
11. Mackintosh, S.F.; Hill, K.D.; Dodd, K.J.; Goldie, P.A.; Culham, E.G. Balance score and a history of falls in hospital predict recurrent falls in the 6 months following stroke rehabilitation. *Arch. Phys. Med. Rehabil.* **2006**, *87*, 1583–1589. [[CrossRef](#)] [[PubMed](#)]
12. Forster, A.; Young, J. Incidence and consequences of falls due to stroke: A systematic inquiry. *BMJ* **1995**, *311*, 83–86. [[CrossRef](#)] [[PubMed](#)]
13. Bloem, B.R.; Grimbergen, Y.A.; Cramer, M.; Willemsen, M.; Zwinderman, A.H. Prospective assessment of falls in Parkinson’s disease. *J. Neurol.* **2001**, *248*, 950–958. [[CrossRef](#)] [[PubMed](#)]
14. Paul, S.S.; Sherrington, C.; Canning, C.G.; Fung, V.S.C.; Close, J.C.T.; Lord, S.R. The relative contribution of physical and cognitive fall risk factors in people with Parkinson’s disease: A large prospective cohort study. *Neurorehabil. Neural Repair* **2014**, *28*, 282–290. [[CrossRef](#)] [[PubMed](#)]
15. Rubenstein, L.Z. Falls in older people: Epidemiology, risk factors and strategies for prevention. *Age Ageing* **2006**, *35*, ii37–ii41. [[CrossRef](#)] [[PubMed](#)]
16. Hendrie, D.; Hall, S.E.; Arena, G.; Legge, M. Health system costs of falls of older adults in Western Australia. *Aust. Health Rev.* **2004**, *28*, 363–373. [[CrossRef](#)] [[PubMed](#)]
17. Stolze, H.; Klebe, S.; Zechlin, C.; Baecker, C.; Friege, L.; Deuschl, G. Falls in frequent neurological diseases—Prevalence, risk factors and aetiology. *J. Neurol.* **2004**, *251*, 79–84. [[CrossRef](#)] [[PubMed](#)]
18. Berg, W.P.; Alessio, H.M.; Mills, E.M.; Tong, C. Circumstances and consequences of falls in independent community-dwelling older adults. *Age Ageing* **1997**, *26*, 261–268. [[CrossRef](#)]
19. Blake, A.J.; Morgan, K.; Bendall, M.J.; Dallosso, H.; Ebrahim, S.B.; Arie, T.H.; Fentem, P.H.; Bassey, E.J. Falls by elderly people at home: Prevalence and associated factors. *Age Ageing* **1988**, *17*, 365–372. [[CrossRef](#)]
20. Begg, R.; Best, R.; Dell’Oro, L.; Taylor, S. Minimum foot clearance during walking: Strategies for the minimisation of trip-related falls. *Gait Posture* **2007**, *25*, 191–198. [[CrossRef](#)]
21. Delfi, G.; Al Bochi, A.; Dutta, T. A scoping review on minimum foot clearance measurement: Sensing modalities. *Int. J. Environ. Res. Public Health* **2021**, *18*, 10848. [[CrossRef](#)] [[PubMed](#)]
22. Schulz, B.W.; Lloyd, J.D.; Lee, W.E. The effects of everyday concurrent tasks on overground minimum toe clearance and gait parameters. *Gait Posture* **2010**, *32*, 18–22. [[CrossRef](#)] [[PubMed](#)]
23. Winter, D.A. Foot trajectory in human gait: A precise and multifactorial motor control task. *Phys. Ther.* **1992**, *72*, 45–56. [[CrossRef](#)] [[PubMed](#)]

24. Smeesters, C.; Hayes, W.C.; McMahon, T.A. Disturbance type and gait speed affect fall direction and impact location. *J. Biomech.* **2001**, *34*, 309–317. [[CrossRef](#)] [[PubMed](#)]
25. Moosabhoy, M.A.; Gard, S.A. Methodology for determining the sensitivity of swing leg toe clearance and leg length to swing leg joint angles during gait. *Gait Posture* **2006**, *24*, 493–501. [[CrossRef](#)]
26. Nagano, H.; Begg, R. A shoe-insole to improve ankle joint mechanics for injury prevention among older adults. *Ergonomics* **2021**, *64*, 1271–1280. [[CrossRef](#)]
27. Begg, R.K.; Tirosch, O.; Said, C.M.; Sparrow, W.A.; Steinberg, N.; Levinger, P.; Galea, M.P. Gait training with real-time augmented toe-ground clearance information decreases tripping risk in older adults and a person with chronic stroke. *Front. Hum. Neurosci.* **2014**, *8*, 243. [[CrossRef](#)]
28. Sarashina, E.; Mizukami, K.; Yoshizawa, Y.; Sakurai, J.; Tsuji, A.; Begg, R. Feasibility of Pilates for late-stage frail older adults to minimize falls and enhance cognitive functions. *Appl. Sci.* **2022**, *12*, 6716. [[CrossRef](#)]
29. Arami, A.; Raymond, N.S.; Aminian, K. An accurate wearable foot clearance estimation system: Toward a real-time measurement system. *IEEE Sens. J.* **2017**, *17*, 2542–2549. [[CrossRef](#)]
30. Santhiranayagam, B.K.; Lai, D.T.H.; Begg, R.K.; Palaniswami, M. Estimation of end point foot clearance points from inertial sensor data. In Proceedings of the 2011 Annual International Conference of the IEEE Engineering in Medicine and Biology Society, Boston, MA, USA, 30 August–3 September 2011; pp. 6503–6506. [[CrossRef](#)]
31. Mariani, B.; Hoskovec, C.; Rochat, S.; Büla, C.; Penders, J.; Aminian, K. 3D gait assessment in young and elderly subjects using foot-worn inertial sensors. *J. Biomech.* **2010**, *43*, 2999–3006. [[CrossRef](#)]
32. Mariani, B.; Rochat, S.; Büla, C.J.; Aminian, K. Heel and toe clearance estimation for gait analysis using wireless inertial sensors. *IEEE Trans. Biomed. Eng.* **2012**, *59*, 3162–3168. [[CrossRef](#)] [[PubMed](#)]
33. Kitagawa, N.; Ogihara, N. Estimation of foot trajectory during human walking by a wearable inertial measurement unit mounted to the foot. *Gait Posture* **2016**, *45*, 110–114. [[CrossRef](#)] [[PubMed](#)]
34. Benoussaad, M.; Sijobert, B.; Mombaur, K.; Coste, C.A. Robust foot clearance estimation based on the integration of foot-mounted IMU acceleration data. *Sensors* **2016**, *16*, 12. [[CrossRef](#)] [[PubMed](#)]
35. Lai, D.T.H.; Charry, E.; Begg, R.; Palaniswami, M. A prototype wireless inertial-sensing device for measuring toe clearance. In Proceedings of the 2008 30th Annual International Conference of the IEEE Engineering in Medicine and Biology Society, Vancouver, BC, Canada, 20–25 August 2008; pp. 4899–4902. [[CrossRef](#)]
36. Asogwa, C.O.; Nagano, H.; Wang, K.; Begg, R. Using deep learning to predict minimum foot-ground clearance event from toe-off kinematics. *Sensors* **2022**, *22*, 6960. [[CrossRef](#)]
37. Prasanth, H.; Caban, M.; Keller, U.; Courtine, G.; Ijspeert, A.; Vallery, H.; von Zitzewitz, J. Wearable sensor-based real-time gait detection: A systematic review. *Sensors* **2021**, *21*, 2727. [[CrossRef](#)] [[PubMed](#)]
38. Kim, J.K.; Bae, M.; Lee, K.B.; Hong, S.G. Gait event detection algorithm based on smart insoles. *ETRI J.* **2020**, *42*, 46–53. [[CrossRef](#)]
39. Köse, A.; Cereatti, A.; Della Croce, U. Bilateral step length estimation using a single inertial measurement unit attached to the pelvis. *J. NeuroEng. Rehabil.* **2012**, *9*, 9. [[CrossRef](#)] [[PubMed](#)]
40. Santhiranayagam, B.K.; Lai, D.T.; Sparrow, W.A.; Begg, R.K. A machine learning approach to estimate Minimum Toe Clearance using Inertial Measurement Units. *J. Biomech.* **2015**, *48*, 4309–4316. [[CrossRef](#)] [[PubMed](#)]
41. Miyake, T.; Fujie, M.G.; Sugano, S. Prediction algorithm of parameters of toe clearance in the swing phase. *Appl. Bionics Biomech.* **2019**, *10*, 4502719. [[CrossRef](#)]
42. Guimarães, V.; Sousa, I.; Correia, M.V. A deep learning approach for foot trajectory estimation in gait analysis using inertial sensors. *Sensors* **2021**, *21*, 7517. [[CrossRef](#)]
43. Lee, S.S.; Choi, S.T.; Choi, S.I. Classification of gait type based on deep learning using various sensors with smart insole. *Sensor* **2019**, *19*, 1757. [[CrossRef](#)] [[PubMed](#)]
44. Mashal, I.; Alsaryrah, O.; Chung, T.Y. Testing and evaluating recommendation algorithms in the internet of things. *J. Ambient Intell. Humaniz. Comput.* **2016**, *7*, 889–900. [[CrossRef](#)]
45. Hasan, S.M.S.; Siddiquee, M.R.; Atri, R. Prediction of gait intention from pre-movement EEG signals: A feasibility study. *J. NeuroEng. Rehabil.* **2020**, *17*, 50. [[CrossRef](#)] [[PubMed](#)]
46. Tsukahara, A.; Hasegawa, Y.; Eguchi, K.; Sankai, Y. Restoration of gait for spinal cord injury patients using HAL with intention estimator for preferable swing speed. *IEEE Trans. Neural Syst. Rehabil. Eng.* **2014**, *23*, 308–318. [[CrossRef](#)] [[PubMed](#)]
47. Novak, D.; Reberšek, P.; De Rossi, S.M.M.; Donati, M.; Podobnik, J.; Beravs, T.; Lenzi, T.; Vitiello, N.; Carrozza, M.C.; Murih, M. Automated detection of gait initiation and termination using wearable sensors. *Med. Eng. Phys.* **2013**, *35*, 1713–1720. [[CrossRef](#)] [[PubMed](#)]
48. XGBoost Documentation. Available online: <https://xgboost.readthedocs.io/en/latest/tutorials/model.html> (accessed on 30 August 2023).
49. Bohannon, R.W.; Wang, Y.C. Four-Meter Gait Speed: Normative Values and Reliability Determined for Adults Participating in the NIH Toolbox Study. *Arch. Phys. Med. Rehabil.* **2019**, *100*, 509–513. [[CrossRef](#)] [[PubMed](#)] [[PubMed Central](#)]
50. Nagano, H. Gait Biomechanics for Fall Prevention among Older Adults. *Appl. Sci.* **2022**, *12*, 6660. [[CrossRef](#)]
51. Nagano, H.; Said, C.M.; James, L.; Sparrow, W.A.; Begg, R. Biomechanical correlates of falls risk in gait impaired stroke survivors. *Front. Physiol.* **2022**, *13*, 833417. [[CrossRef](#)] [[PubMed](#)] [[PubMed Central](#)]

52. Al Bochi, A.; Delfi, G.; Dutta, T. A scoping review on minimum foot clearance: An exploration of level-ground clearance in individuals with abnormal gait. *Int. J. Environ. Res. Public Health* **2021**, *18*, 10289. [[CrossRef](#)] [[PubMed](#)] [[PubMed Central](#)]
53. Seaborn. Available online: <https://seaborn.pydata.org> (accessed on 15 October 2022).
54. Derlatka, M. Modified kNN algorithm for improved recognition accuracy of biometrics system based on gait. In *IFIP International Conference on Computer Information Systems and Industrial Management*; Springer: Berlin/Heidelberg, Germany, 2013; pp. 59–66.
55. Gupta, A.; Jadhav, A.; Jadhav, S.; Thengade, A. Human gait analysis based on decision tree, random forest and KNN algorithms. In *Applied Computer Vision and Image Processing*; Springer: Singapore, 2020; pp. 283–289.
56. Rattanasak, A.; Uthansakul, P.; Uthansakul, M.; Jumphoo, T.; Phapatanaburi, K.; Sindhupakorn, B.; Rooppakhun, S. Real-Time Gait Phase Detection Using Wearable Sensors for Transtibial Prosthesis Based on a kNN Algorithm. *Sensors* **2022**, *22*, 4242. [[CrossRef](#)] [[PubMed](#)] [[PubMed Central](#)]
57. Qiu, J.G.; Li, Y.; Liu, H.Q.; Lin, S.; Pang, L.; Sun, G.; Song, Y.Z. Research on motion recognition based on multi-dimensional sensing data and deep learning algorithms. *Math. Biosci. Eng.* **2023**, *20*, 14578–14595. [[CrossRef](#)] [[PubMed](#)]
58. Halim, N. Stochastic recognition of human daily activities via hybrid descriptors and random forest using wearable sensors. *Array* **2022**, *15*, 100190. [[CrossRef](#)]
59. Gao, J.; Ma, C.; Wu, D.; Xu, X.; Wang, S.; Yao, J. Recognition of human motion intentions based on Bayesian-optimized XGBOOST algorithm. *J. Sens.* **2022**, 1–15. [[CrossRef](#)]
60. Kranzinger, C.; Bernhart, S.; Kremser, W.; Venek, V.; Rieser, H.; Mayr, S.; Kranzinger, S. Classification of human motion data based on inertial measurement units in sports: A scoping review. *Appl. Sci.* **2023**, *13*, 8684. [[CrossRef](#)]
61. Kuhn, M.; Johnson, K. *Applied Predictive Modeling*; Springer: New York, NY, USA, 2013.
62. Kuhn, M. Futility Analysis in the Cross-Validation of Machine Learning Models. *arXiv* **2014**, arXiv:1405.6974.
63. Fisher, A.; Rudin, C.; Dominici, F. All models are wrong, but many are useful: Learning a variable’s importance by studying an entire class of prediction models simultaneously. *arXiv* **2018**, arXiv:1801.01489.
64. Kuhn, M.; Johnson, K. Measuring Performance in Classification Models. In *Applied Predictive Modeling*; Springer: New York, NY, USA, 2013; pp. 247–273. [[CrossRef](#)]
65. Saito, T.; Rehmsmeier, M. The precision-recall plot is more informative than the ROC plot when evaluating binary classifiers on imbalanced datasets. *PLoS ONE* **2015**, *10*, e0118432. [[CrossRef](#)] [[PubMed](#)]
66. Mills, P.M.; Barrett, R.S. Swing phase mechanics of healthy young and elderly men. *Hum. Mov. Sci.* **2001**, *20*, 427–446. [[CrossRef](#)]
67. Kubota, S.; Kadone, H.; Shimizu, Y.; Koda, M.; Noguchi, H.; Takahashi, H.; Watanabe, H.; Hada, Y.; Sankai, Y.; Yamazaki, M. Development of a new ankle joint hybrid assistive limb. *Medicina* **2022**, *58*, 395. [[CrossRef](#)]
68. Sankai, Y. HAL: Hybrid Assistive Limb Based on Cybernetics. In *Robotics Research. Springer Tracts in Advanced Robotics*; Kaneko, M., Nakamura, Y., Eds.; Springer: Berlin/Heidelberg, Germany, 2010; Volume 66.
69. Soma, Y.; Kubota, S.; Kadone, H.; Shimizu, Y.; Takahashi, H.; Hada, Y.; Koda, M.; Sankai, Y.; Yamazaki, M. Hybrid Assistive Limb Functional Treatment for a Patient with Chronic Incomplete Cervical Spinal Cord Injury. *Int. Med. Case Rep. J.* **2021**, *14*, 413–420. [[CrossRef](#)]
70. Mataka, Y.; Kamada, H.; Mutsuzaki, H.; Shimizu, Y.; Takeuchi, R.; Mizukami, M.; Yoshikawa, K.; Takahashi, K.; Matsuda, M.; Iwasaki, N.; et al. Use of Hybrid Assistive Limb (HAL[®]) for a postoperative patient with cerebral palsy: A case report. *BMC Res. Notes* **2018**, *11*, 201. [[CrossRef](#)] [[PubMed](#)]

Disclaimer/Publisher’s Note: The statements, opinions and data contained in all publications are solely those of the individual author(s) and contributor(s) and not of MDPI and/or the editor(s). MDPI and/or the editor(s) disclaim responsibility for any injury to people or property resulting from any ideas, methods, instructions or products referred to in the content.